Canadian Mineralogist
Vol. 27, pp. 15-22 (1989)

COMPUTER-AIDED DETERMINATION OF CRYSTAL-LATTICE ORIENTATION FROM ELECTRON-CHANNELING PATTERNS IN THE SEM

NIELS-HENRIK SCHMIDT* AND NIELS Ø. OLESEN
Geologisk Institut, Aarhus Universitet, C.F. Møllers Allé, DK-8000 Aarhus C, Denmark

ABSTRACT

The paper presents the major steps of a mathematical procedure that permits the simulation of Electron Channeling Pattern (ECP) maps of any mineral species for which unit-cell constants, the atomic species and their equivalent positions are known. The basis of calculation is the Bragg equation, the structure factor *F*, and the atomic scattering factors of the atomic species. Simulated spherical ECP maps for chromite and quartz are presented and compared to traditional ECP maps, which were constructed from ECP photomicrographs, with good results. The fraction of the ECP sphere that covers all possible orientations of a crystal is discussed for all 32 point groups. It is shown that Laue-group symmetry is the determining factor, which results in a loss of "resolution" in certain point groups. The ECP simulation leads to the creation of a software package CHANNEL, which permits rapid ECP-pattern recognition and lattice-orientation determination, in principle without the need for previous construction of an ECP map.

Keywords: scanning electron microscopy, electron-channeling pattern, computer simulation, electron-diffraction intensity, lattice-orientation determination, software package.

SOMMAIRE

Nous présentons ici les étapes importantes d'une procédure mathématique qui reproduit les schémas de canalisation des électrons (SCE) de toute espèce minérale pour laquelle les paramètres réticulaires, les sortes d'atomes, et leurs positions équivalentes sont connus. À la base de ces calculs sont l'équation de Bragg, les facteurs de structure F, et les coefficients de dispersion des atomes impliqués. Des cartes des schémas de canalisation sphériques pour chromite et quartz ressemblent aux cartes traditionnelles, construites à partir de photomicrographies SCE. Il est question de la fraction de la sphère SCE qui couvre toutes les orientations possibles d'un cristal, pour chacun des 32 groupes ponctuels. La symétrie du groupe de Laue est le facteur important, ce qui cause une perte de résolution pour certains groupes ponctuels. La simulation SCE mène à l'élaboration du logiciel CHANNEL, qui permet de reconnaître rapidement les schémas de canalisation des électrons et l'orientation du réseau dans chaque cas, en principe sans l'aide d'une carte SCE élaborée à la suite de constructions antérieures.

(Traduit par la Rédaction)

Mots-clés: microscopie électronique à balayage, schéma de canalisation des électrons, simulation par ordinateurs, intensité de la diffraction des électrons, détermination de l'orientation du réseau, logiciel.

INTRODUCTION

Since Coates (1967) observed the first electron-channeling pattern (ECP) in the scanning electron microscope (SEM), numerous investigators have described aspects of the technique and its potential in the study of crystalline materials (Joy *et al.* 1982, and references therein). The most outstanding feature is the ability to determine crystal-lattice orientation with a precision of ~0.5° from areas a few micrometers in diameter, whilst fully maintaining the microstructural context of this information. Lloyd *et al.* (1981) first applied the technique to geological materials; since then, a number of studies have appeared (Christiansen 1986, Lloyd & Ferguson 1986, Ferguson *et al.* 1987, Lloyd *et al.* 1987a,b).

The basic physical principles behind the technique are as follows (*e.g.*, Newbury & Yakowitz 1975): an electron beam, accelerated in the SEM, strikes the surface of the study material and penetrates it; owing to elastic scattering events, a fraction of the electrons returns to the surface. If the material is crystalline, the lattice "channels" the electrons during this process, and the emission of electrons from the surface of the specimen is a function of the geometry between the electron beam and the lattice planes. If the electron beam strikes the specimen surface at various angles (the beam is said to be "rocking"), the emitted electrons are transformed by the detector system to an image built up by contrast lines and bands, the geometry of which reflects the orientation of the specimen's crystal lattice. The surface of the specimen must be flat, free of defects, and clean, otherwise the lattice-dependent information will be "overprinted" by contrast effects arising from variations in topography or will be lost in the general reduction of the backscattering contrast. For this reason, most geological specimens require special polishing (Lloyd 1987).

Hitherto, the determination of lattice orientation has proceeded by means of one of the following methods: 1) a visual comparison of the ECP image with an ECP map, which is either a computer-drawn

*Present address: Forskningscenter Risø, Postboks 49, 4000 Roskilde, Denmark.

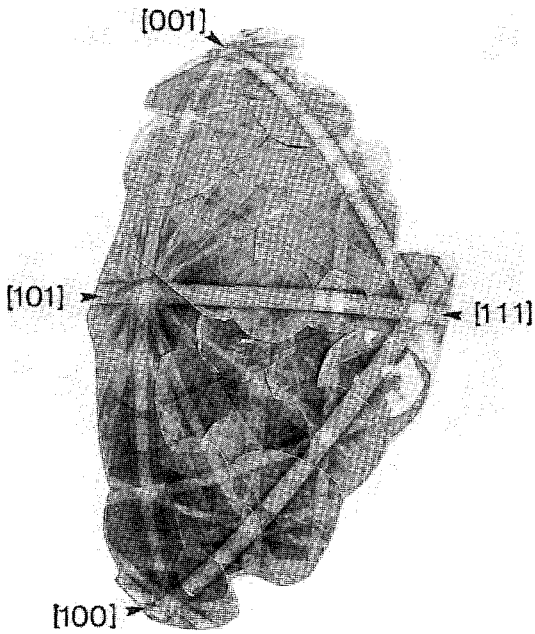

FIG. 1. Spherical ECP map of chromite; 35 kV accelerating voltage.

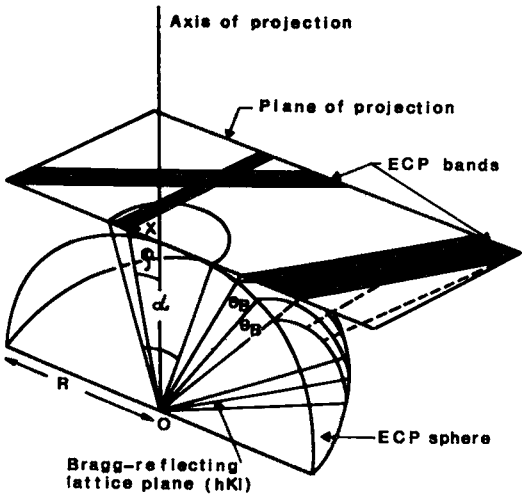

FIG. 2. The ECP sphere. A Bragg-reflecting lattice plane (*hkl*) is projected onto the plane using the gnomonic projection ($X = R * \tan \varphi$). Further explanation is given in the text.

pattern (*e.g.*, Young & Lytton 1972) or a mosaic constructed from SEM/ECP photomicrographs covering all possible orientations of the crystal lattice (Joy *et al.* 1982). The ECP map may be two-dimensional, or better still, constructed on the surface of a sphere (*e.g.*, Lloyd & Ferguson 1986). 2) Calculation based on dimensions and angles between the contrast lines in the ECP image (*e.g.*, Kozubowski *et al.* 1987, Weiland & Schwarzer 1986).

Lattice-orientation determination by means of a visual comparison of the ECP image with an ECP map is a tedious procedure, especially where a lattice of low symmetry is concerned. Firstly, the construction of the ECP mosaic map itself demands a large number of polished sections, cut variably and systematically from a single crystal [33 specimens were used by Lloyd & Ferguson (1986) to obtain the full range of ECP photomicrographs for quartz], or alternatively, the required number of ECP photomicrographs can be obtained randomly from a polycrystalline specimen (we used approximately 30 photomicrographs to construct the spherical ECP map for chromite: Fig. 1). Secondly, these photomicrographs must be fitted and glued together on the surface of the sphere, which greatly impairs the reproducibility of the map. Thirdly, the identification of the ECP image of unknown orientation is time-consuming. Fourthly, the measurement of the spherical angles, which specify the orientation of the lattice (ECP image), is done by hand with curved rulers (*e.g.*, Lloyd & Ferguson 1986), and may not always be accurate.

The purpose of this paper is to describe the major steps of a mathematical procedure that permits the construction of spherical ECP maps of any mineral species, with the aid of a microcomputer. As a new feature, the electron-diffraction intensity is also displayed. The procedure results in the construction of a computer model and the simulation of ECP patterns, including contrast variations. This permits rapid ECP image recognition and calculation of relevant spherical angles such as Euler angles (Baker & Wenk 1972).

BASIS OF CALCULATIONS

The ECP pattern is described by a number of bands, each characterized by its width, contrast with respect to the background, and orientation (Fig. 1). In the following, it is assumed that the electron beam of the SEM can be treated as photons, and that the bands are due to diffraction, satisfying the Bragg equation:

$$\lambda = 2d_{hkl} \sin \theta_B \quad (1)$$

where d_{hkl} is the distance between lattice planes, and θ_B is the Bragg angle.

The De Broglie wavelength (λ, in Ångströms) for an electron accelerated in a potential field (V in eV) is given by the relation (Alonso & Finn 1979):

$$\lambda = 12.3 / \sqrt{V} \quad (2)$$

Consider a sphere with its origin in a crystal lattice. Assume that all lattice planes contain the origin, and let those lattice planes that are Bragg-reflecting cut the surface of the sphere to produce a number of great-circles. However, each great-circle is represented by two small-circles, symmetrically positioned on either side of the great-circle and separated from it by the Bragg angle (θ_B) distance (Fig. 2). It is a basic assumption that these small-circles are equivalent to the ECP band margins, and that the width of an ECP band is proportional to twice the Bragg angle for the lattice plane in question (*e.g.*, Joy *et al.* 1982), and therefore, as given by Eq. 1, inversely proportional to the distance d_{hkl} between lattice planes. The distance between lattice planes is a function of the cell constants, and they may be read as functions of indices in, for example, Bloss (1971, p. 467). Lattice planes with higher indices generally have smaller d_{hkl} and, consequently, larger ECP band widths (Eq. 1).

The intensity of a Bragg-reflecting lattice plane is approximately proportional to the square of the structure factor F. The structure factor is a complex number that is a function of the atomic species in the lattice and their relative position in the unit cell. F is calculated for lattice plane (hkl) from the expression (Sands 1975, p. 106):

$$F(hkl) = \Sigma f_j \exp[2\pi i(hx_j + ky_j + lz_j)] \qquad (3)$$

where $(xyz)_j$ is the relative position of atom j, and f_j is the atomic scattering factor of atom j in the unit cell. The summation is carried out over all atoms in the unit cell. The atomic scattering factor f is a function of d_{hkl}; it is tabulated in International Tables for X-ray Crystallography. F^2 generally decreases with increasing lattice-plane indices. The orientation of the Bragg-reflecting lattice planes is calculated by applying the concept of the reciprocal lattice and well-known techniques of vector and matrix calculation (*e.g.*, Young & Lytton 1972).

It is now possible to create a computer model of the ECP sphere for any mineral species of known unit-cell constants, atomic species and their symmetry-equivalent positions. This model contains the orientation of all Bragg-reflecting lattice planes, their associated relative band-width, and relative intensities of reflection.

Pattern Symmetry of the ECP Sphere

As a consequence of Friedel's Law, the backscattering of electrons in any crystal is identical for opposite directions. This means that the diffraction pattern on the ECP sphere must display a center of symmetry, whether the crystal has one or not. Therefore, rather than using point-group symmetry, it is necessary to use Laue-group symmetry, which reflects both the symmetry of the crystal and the centrosymmetry intrinsic to the ECP technique. This reduces the 32 point groups to 11 Laue groups (Table 1). The effect of the centrosymmetry on the pattern of the ECP sphere is that mirror images are displayed for opposite directions (Fig. 3). It is therefore possible to distinguish between opposite directions in any crystal unless the direction is parallel to a mirror plane. In the latter case, identical images appear because of the additional element of symmetry.

TABLE 1. THE 11 LAUE GROUPS AND THE ASSOCIATED 32 POINT GROUPS#

$\bar{1}$	$2/m$	mmm	$4/m$	$4/mmm$		
1	m*	$mm2$*	$\bar{4}$*	$\bar{4}2m$*		
	2	222	4	$4mm$*		
				422		
$\bar{3}$	$\bar{3}m$	$6/m$	$6/mmm$	$m3$	$m3m$	
3	$3m$*	$\bar{6}$*	$\bar{6}m2$*	23	$\bar{4}3m$*	
	32	6	$6mm$*		432	
			622			

The symbol of each Laue group is adopted from the holosymmetrical point-group (underlined). * The point groups in which the ECP technique has a reduced "resolution", compared to the crystal symmetry as it is expressed through the point-group symmetry.

The fraction of the ECP sphere necessary to cover all possible ECP images, henceforth called "the elementary pattern of the ECP sphere" (EPS), can be deduced by applying the Laue-group elements of symmetry to an ECP image in a general position. The result of the analysis is shown in Figure 4 for all 11 Laue groups. The size of the EPS is unambiguous, and it is inversely proportional to the number of identical ECP images, but the position of the EPS on the ECP sphere may have several equivalent solutions.

All Laue groups are subdivided according to point groups in Table 1. A comparison of Laue-group symmetry with point-group symmetry reveals the possibility of reduction by half of the size of the EPS. This is the case in 10 of 32 point groups (marked with a star in Table 1); where this occurs, the number of equivalent solutions to the lattice orientation is dou-

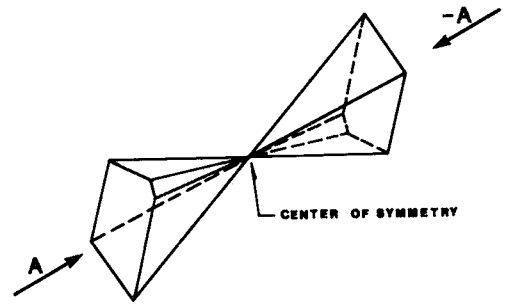

FIG. 3. The "Friedel's Law" effect on an ECP pattern. Because of the center of symmetry, mirror images are observed from opposite directions (A and -A).

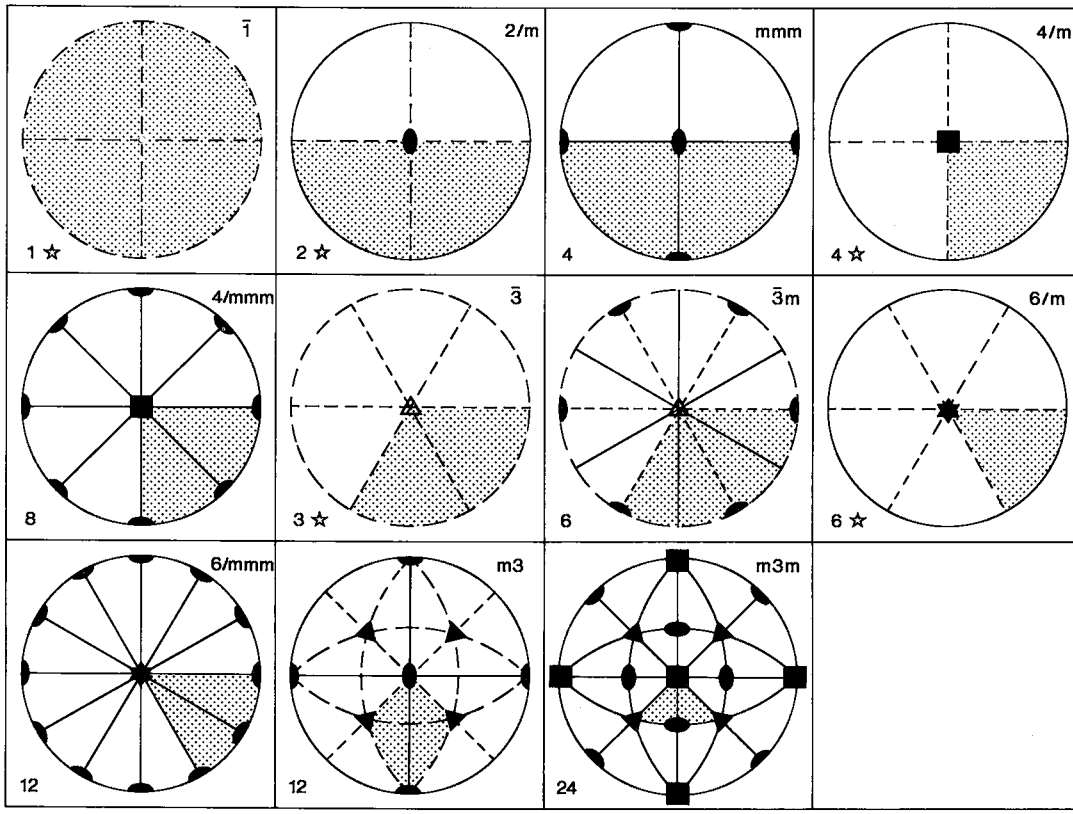

FIG. 4. Stereographic projections of the 11 Laue symmetry groups, displaying "the elementary pattern of the ECP sphere" (EPS) (ornamented). The symbol of the Laue group is indicated in the upper right corner. The number of identical ECP patterns for an arbitrary lattice direction, and thereby the size of the EPS, is shown in the lower left corner. A star denotes that the EPS covers both the upper and the lower hemisphere. Further explanation is given in the text.

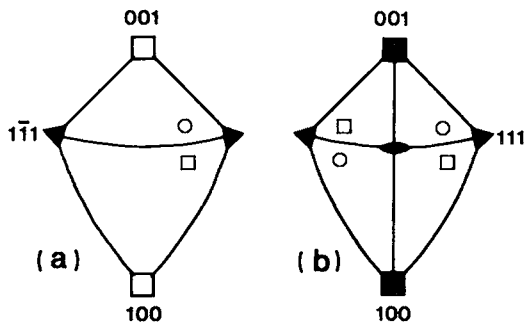

FIG. 5. a) A fraction of the crystallographic stereogram for the point group $\bar{4}3m$; b) a similar fraction of the stereogram for the Laue group $m3m$. The circle represents an object with no internal symmetry, and the square represents the mirror image of this object.

bled, thereby lowering the "resolution" of the technique. As an example, sphalerite belongs to the point group $\bar{4}3m$ and the Laue group $m3m$, which reduces the size of the EPS from 1/12 to 1/24 of the surface of sphere. This means that sphalerite crystals of different orientation may display identical ECP images and are therefore indistinguishable (Fig. 5).

PROJECTIONS OF THE ECP SPHERE

An ECP image is displayed on a two-dimensional surface, *viz.* a video screen (SEM/CRT), or photographic paper. Therefore, the small-circles of the ECP sphere must be projected onto a plane (Fig. 2). We use the gnomonic projection here because of simplicity in calculation and geometry. However, the choice of projection is not critical because the "rocking" of the electron beam in SEM/ECP mode typi-

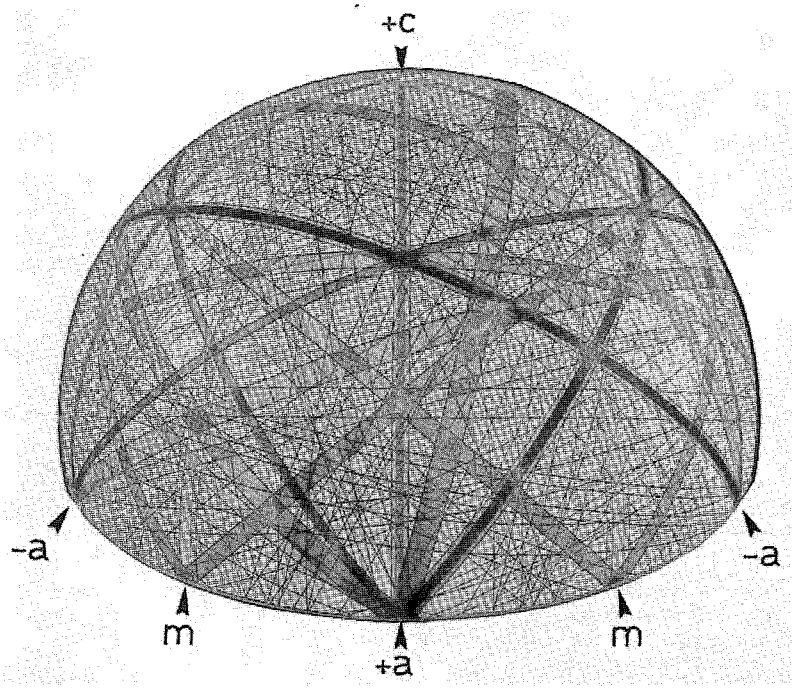

FIG. 6. Computer-simulated spherical ECP map of quartz of point group 32 (alpha, right-handed); 30 kV accelerating voltage.

cally is $\pm 10°$ or less. This means that we are interested only in that part of the projection plane that is inside a cone of 20° opening angle, with the axis of projection as the cone axis (Fig. 2). The stereographic, the gnomonic, and the orthographic projections all yield almost identical results.

One option we considered was to construct a visualization of the ECP sphere, analogous to the spherical ECP map, by fitting together a large number of such simulated ECP images on the surface of a sphere of radius R (Fig. 2). We have, however, adopted a different approach for technical reasons. Fitting plane paper to a doubly curved surface leads to distortion of the paper. Old-fashioned globes overcome this distortion by gluing narrow strips to the globe along the meridian of longitude. We have therefore constructed a special projection for this purpose in which "the plane of projection" is singly curved (cylindrical), touching the ECP sphere along a great-circle.

Figure 6 is such a simulated spherical ECP map of quartz (alpha, right-handed), and Figure 7a displays a similar map for chromite. In both cases sections of 5° width are used, giving very small distortions. To avoid a complete mesh of small-circles on the maps, only lattice planes of higher Bragg-reflection intensities are plotted; in this case a cut-off limit of $I/I_{max} = 5\%$ is adopted. We have added a commercial raster to indicate the calculated relative intensities of Bragg reflection. The darkest raster indicates a relative reflection greater than 70%, whereas the lightest indicate between 10 and 20% of maximum reflection.

A comparison of the simulated ECP maps with the spherical ECP maps constructed from photomicrographs (chromite in Fig. 7a and Fig. 1, quartz in Fig. 6; also Fig. 5 in Lloyd & Ferguson 1986) demonstrates so many and highly accurate similarities that we may confidently assert the computer-model's reliability. However, there are occasional deviations between the model and micrograph, not in the orientation of the bands and their widths, but in the calculated intensity of Bragg reflections. This may be observed in cases of "multiple" bands, such as Bragg reflections from $\{01\bar{1}1\}$ and $\{02\bar{2}2\}$ in quartz.

LATTICE-ORIENTATION DETERMINATION BY THE COMPUTER MODEL

The comparison between the SEM-generated ECP map and the computer-generated ECP map demonstrates the model's reliability, especially with regards to ECP band orientation and width. This makes it possible to achieve a computer-aided recognition of the orientation of any ECP photomicrograph, *i.e.*, its position on the spherical ECP map.

Any ECP image displays a unique combination

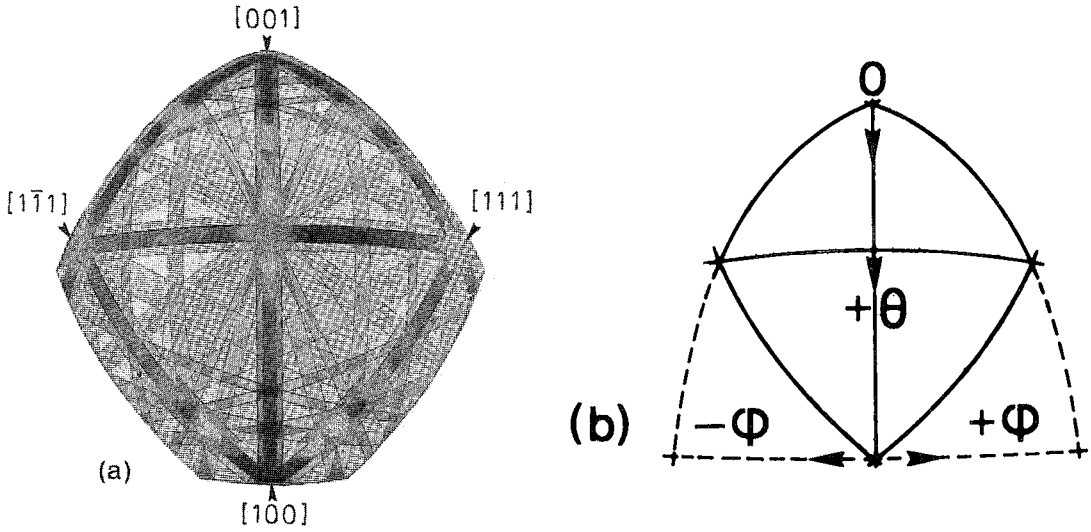

FIG. 7. a) Computer-simulated spherical ECP map of chromite of point group *m*3*m;* 30 kV accelerating voltage. Note that the map is twice the size of "the elementary pattern of the ECP sphere" (EPS), whereas the map of Figure 1 is the correct size, but is positioned differently from the EPS of Figure 4. b) Spherical angles used to describe the position of an ECP image on the ECP map (see Fig. 8).

of angles between bands and their widths; we have created a software package (CHANNEL) that takes advantage of this fact. The position of the margins of three bands, which do not intersect at one point, are entered into the microcomputer using a digitizer table (Fig. 8b). Through the gnomonic projection, each ECP band is turned into a three-dimensional (lattice) plane with the associated lattice spacing, d_{hkl}, calculated from the band width. This information is matched against the orientation and spacing of the lattice planes known from the theoretical calculations. In mathematical terms, a successful matching is expressed by the following matrix equation:

$$T = M(\mathrm{c}) * M^{-1}(r) \qquad (4)$$

where M(c) denotes the three lattice planes as they are calculated from the specification of the crystal structure, $M(r)$ the same three lattice planes as they are measured from the ECP image, and T is the rotation matrix, which expresses the orientation of the crystal (c) relative to a reference system (r).

The gnomonic projection of the position on the ECP sphere, which is in accordance with T, is displayed for visual inspection (Fig. 8c); a final fine-scale adjustment (translation, rotation) of the position on the ECP sphere is often necessary owing to computational round-offs. Spherical angles used for graphical representation of ECP data (*e.g.*, Lloyd 1987) are calculated with high precision and displayed in the desired projection (pole figure, inverse pole figure).

DISCUSSION AND CONCLUSION

We have presented the basic aspects of a computer model for ECP pattern generation and recognition. A crucial feature is the ability to perform a lattice-orientation determination without any previous knowledge of the ECP pattern, by a simple visual comparison. The reasons of the occasional deviations between the observed and computed intensities of Bragg reflections are under investigation. It should be stressed, however, that the mismatch in no way invalidates the model; ECP pattern recognition is still an accurate and simple procedure. We intend to make improvements of the theoretical model by a feedback technique where the observed relative Bragg-reflection intensities are incorporated into the model.

A typical petrofabric study involves determination of the orientation of 300–500 grains in the material concerned, which with the optical microscope and U-stage technique commonly takes a few minutes per grain. With CHANNEL, we perform an orientation determination from a photomicrograph typically within one minute. As yet, the most time-consuming aspects are specimen preparation and SEM operation. To improve the speed of the technique, it is clearly necessary to interface the SEM with a microcomputer and to use automated pattern-

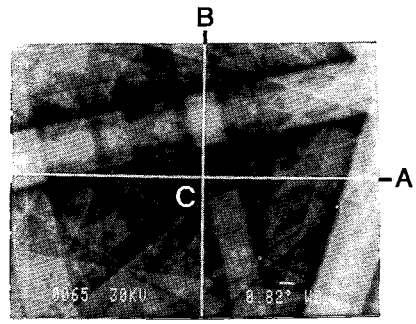

(a)

CHANNEL DIGITALIZE Chromite maxB=42 minI=5 N=184

COMMAND >>> plot band - 3
bandmargin nr. 2
points pr.margin= 5 (2<=number<=20)

RESfile:
Records:
Last:

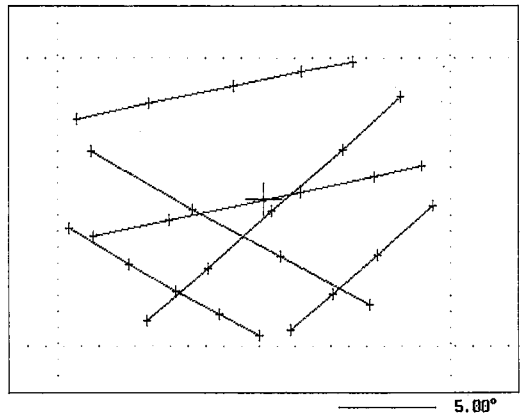

F1=Resultfile
F2=Accell. and scale
F3=Look-through keys
F4=Micrograph rotat.
F5=Screen/Micrograph
F6=Sound

(b)

Radius(mm)= 386.89
Qfactor= 1.13
Screen/Mic.=

CHANNEL DIGITALIZE Chromite maxB=42 minI=5 N=184

COMMAND >>> calculations

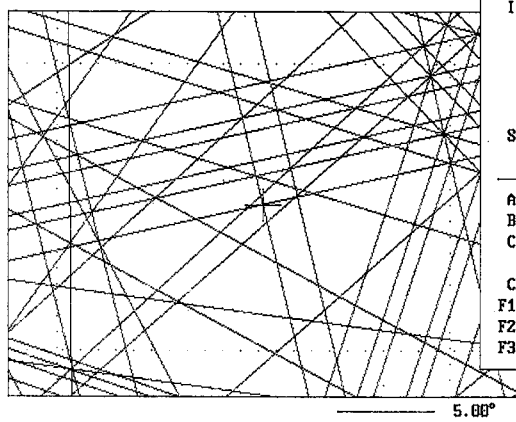

Solution

Likely solut. 0
Iteration: 1

Band 1: 8 0 -8
Band 2: 8 4 -4
Band 3: 3 -5 -5

Spherical coordinates
θ φ

A: 97.6 -117.1
B: 136.4 -19.1
C: 47.5 -34.2

CR/+/- yes/likely/no
F1 quit this image
F2 show likely sol.
F3 min.-intensity 8.8

(c)

FIG. 8. Example of ECP indexing using the computer model. a) ECP photomicrograph of chromite, with reference axes A, B, and C. b) CHANNEL screen after entering the margins of 3 ECP bands (6 lines) into the microcomputer *via* the digitizer table. c) CHANNEL screen after identification of the correct position on the ECP sphere. The spherical angles (Fig. 7b) that describe the orientations of the reference axes A, B, and C are displayed at the right.

recognition techniques.

Compared with the closely related Electron Back Scattering (EBS) technique (*e.g.*, Dingley 1984), the spatial resolution of the ECP technique is relatively small, since the BSE technique is characterized by a submicrometer spot-size owing to a stationary beam and low beam-current. However, the EBS technique suffers from the fact that direct observation of the microstructure during the lattice-orientation measurements is impeded because of the required geometry between beam and specimen (the surface of the specimen is tilted more than 60° relative to the beam). Consequently, the ECP technique is advantageous in many applications where a very high spatial resolution is not important. The technique is applicable in principle to all kinds of minerals. The technique is discrete and nondestructive; with assistance from an appropriate software, it quickly yields "high-quality" lattice-orientation determinations with a precision of better than 0.5 degrees.

Acknowledgements

G.E. Lloyd contributed with many discussions and suggested improvements of the manuscript; D. Herfort improved the English text, and L. Jans and J. Kjeldsen gave technical assistance. The study was supported by the Danish Natural Science Research Council (11-4715, 11-5333, 11-6543).

References

Alonso, M. & Finn, E.J. (1979): *Fundamental University Physics. III. Quantum and Statistical Physics.* Addison-Wesley, Reading, Mass.

Baker, D.W. & Wenk, H.R. (1972): Preferred orientation in a low-symmetry quartz mylonite. *J. Geol.* **80**, 81-105.

Bloss, F.D. (1971): *Crystallography and Crystal Chemistry.* Holt & Rinehart, New York.

Christiansen, F.G. (1986): Deformation of chromite: S.E.M. investigations. *Tectonophys.* **121**, 175-196.

Coates, D.G. (1967): Kikuchi-like reflection patterns obtained with the scanning electron microscope. *Phil. Mag.* **16** (Ser. **8**), 1179-1184.

Dingley, D.J. (1984): Diffraction from sub-micron areas using electron backscattering in a scanning electron microscope. *Scanning Electron Microsc.* **II**, 569-575.

Ferguson, C.C., Lloyd, G.E. & Knipe, R.J. (1987): Fracture mechanics and deformation processes in natural quartz: a combined Vickers indentation, SEM, and TEM study. *Can. J. Earth Sci.* **24**, 544-555.

Joy, D.C., Newbury, D.E. & Davidson, D.L. (1982): Electron channeling patterns in the scanning electron microscope. *J. Appl. Phys.* **53**, 81-122.

Kozubowski, J.A., Ji Lii, M. & Gerberich, W.W. (1987): On some practical aspects of orientation determination using electron channeling patterns. *Scanning* **9**, 237-247.

Lloyd, G.E. (1987): Atomic number and crystallographic contrast images with the SEM: a review of backscattered electron techniques. *Mineral. Mag.* **51**, 3-19.

_____ & Ferguson, C.C. (1986): A spherical electron channeling pattern map for use in quartz petrofabric analysis. *J. Struct. Geol.* **8**, 517-526.

_____, _____ & Law, R.D. (1987a): Discriminatory petrofabric analysis of quartz rocks using SEM electron channelling. *Tectonophys.* **135**, 243-249.

_____, Hall, M.G., Cockayne, B. & Jones, D.W. (1981): Selected area electron channeling patterns from geological materials: specimen preparation, indexing and representation of patterns and applications. *Can. Mineral.* **19**, 505-518.

_____, Law, R.D. & Schmid, S.M. (1987b): A spherical electron channeling pattern map for use in quartz petrofabric analysis: correction and verification. *J. Struct. Geol.* **9**, 251-253.

Newbury, D.E. & Yakowitz, H. (1975): Contrast mechanisms of special interest in materials science. *In* Practical Scanning Electron Microscopy: Electron and Ion Microprobe Analysis (J.I. Goldstein & H. Yakowitz, eds.). Plenum Press, New York.

Sands, D.E. (1975): *Introduction to Crystallography.* W.A. Benjamin, Inc., London.

Weiland, H. & Schwarzer, R. (1986): Online texture determination by Kikuchi or channeling patterns. *In* Experimental Techniques of Texture Analysis (H.J. Bunge, ed.). Deutsche Gesellschaft für Metallkunde, Oberursel.

Young, C.T. & Lytton, J.L. (1972): Computer generation and identification of Kikuchi projections. *J. Appl. Phys.* **43**, 1408-1417.

Received November 5, 1987, revised manuscript accepted April 18, 1988.

Appendix

The software package CHANNEL is written for an IBM or compatible microcomputer (640 kb RAM). A Math coprocessor is advantageous. The graphical resolution may be any of the following international standards: CGA, Olivetti, Hercules, VGA and EGA. With VGA and EGA, the calculated diffraction intensities can be displayed with the use of a grey-scale monitor. CHANNEL will be commercially available in 1988.